

Cite this: *Chem. Sci.*, 2019, 10, 1419

All publication charges for this article have been paid for by the Royal Society of Chemistry

Received 20th September 2018
Accepted 14th November 2018

DOI: 10.1039/c8sc04188a

rsc.li/chemical-science

Catalytic farming: reaction rotation extends catalyst performance†

Ayda Elhage,^{ID} Anabel E. Lanterna^{ID*} and Juan C. Scaiano^{ID*}

The use of heterogeneous catalysis has key advantages compared to its homogeneous counterpart, such as easy catalyst separation and reusability. However, one of the main challenges is to ensure good performance after the first catalytic cycles. Active catalytic species can be inactivated during the catalytic process leading to reduced catalytic efficiency, and with that loss of the advantages of heterogeneous catalysis. Here we present an innovative approach in order to extend the catalyst lifetime based on the crop rotation system used in agriculture. The catalyst of choice to illustrate this strategy, Pd@TiO₂, is used in alternating different catalytic reactions, which reactivate the catalyst surface, thus extending the reusability of the material, and preserving its selectivity and efficiency. As a proof of concept, different organic reactions were selected and catalyzed by the same catalytic material during target molecule rotation.

Introduction

The industrial production of fine chemicals has led to the development of a plethora of different catalysts, many based on Pd complexes.¹ Although many industrial applications utilize homogeneous Pd complexes, heterogeneous Pd metal-based systems are finding their place among industrial processes. The advantages of heterogeneous systems over their homogeneous counterparts are related to the ease of separation and reusability of the materials.² Further, an increased interest in improved understanding of the catalytic activity of heterogeneous materials has led to exciting developments in the field.³ However, the deactivation of heterogeneous catalysts is a ubiquitous problem, yet to be resolved.⁴ Particularly in the petroleum industry, many sacrificial oxidative or reductive processes are utilized in order to extend the catalytic activity, and in the process to decrease the quantities of spent petroleum catalysts.⁵ Our contribution deals with smaller scale production, as it may be applicable to pharmaceuticals, fine chemicals and high value added organic synthesis. We have previously reported on Pd-decorated TiO₂,^{6–8} a versatile material that can be used for different organic transformations, showing variable catalyst longevity. In order to develop sustainable recovery strategies, we propose a strategy based on a reaction rotation methodology, a method we label catalytic farming due to its resemblance to agricultural practices.^{9,10} As it is well-known in agriculture, the

continuous use of the same crop can reduce the content of certain nutrients in the soil, thus reducing the soil yield. With crop rotation, farmers ensure that the nutrients leached or restored by one crop can be absorbed by the following one in the next growing season. The same idea can be extrapolated to catalysis: one reaction can deplete the catalyst of certain properties that can be restored by another reaction during the next catalytic cycle. The ability to reuse catalysts is consistent with the principles of green chemistry, which encourages the use of sustainable practices.¹¹

Results and discussion

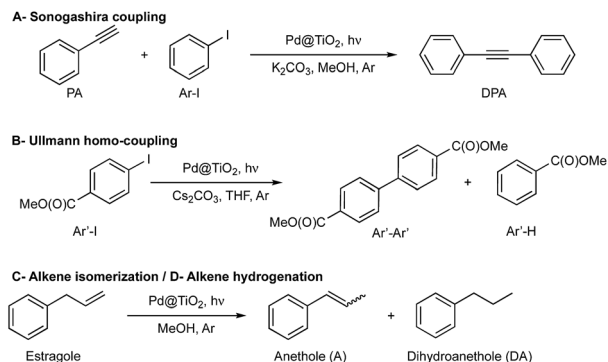
In this work, we demonstrate that rotating the catalytic processes to synthesize alternating target molecules achieves these goals. Just as retaining the properties and richness of the soil is key to agriculture, having a robust catalyst able to perform many catalytic cycles is essential for their efficient and prolonged application in organic synthesis.

Our choice of catalyst to illustrate our rotation strategy is palladium nanoparticles (~1.3 nm, 2 wt%) deposited on nanometric TiO₂ (Pd@TiO₂), predominantly in its anatase form, a catalyst that we have utilized for several organic transformations,^{6–8} including C–C coupling reactions (Ullmann homo-coupling and Sonogashira coupling).^{6,7} These are among the examples we use to illustrate the catalytic farming concept, along with alkene isomerization (or hydrogenation)⁸ also described in this contribution (Scheme 1). We based our reaction selection on previous mechanistic studies that include the role of the solvent and evaluation of the catalyst after each reaction. Thus, while catalytic Sonogashira reaction deteriorates rapidly with usage (problem reaction), catalytic Ullmann

Department of Chemistry and Biomolecular Sciences, Centre for Advanced Materials Research (CAMaR), University of Ottawa, 10 Marie Curie, Ottawa, Ontario K1N 6N5, Canada. E-mail: jscaiano@uottawa.ca; alantern@uottawa.ca

† Electronic supplementary information (ESI) available: TEM catalyst characterization, graphs of conversions and yields and multiple product tables for several reaction rotations. See DOI: 10.1039/c8sc04188a

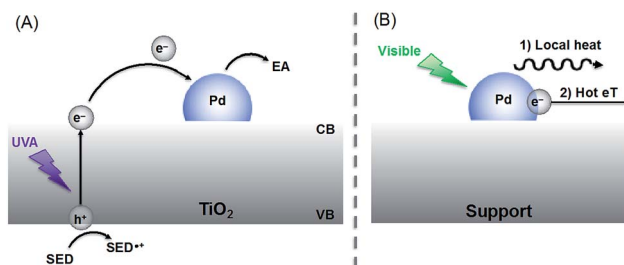




Scheme 1 Reactions used to demonstrate the catalytic farming concept. (A) Sonogashira coupling⁷ is catalyzed by supported PdNP upon visible light irradiation in methanol (MeOH) and Ar atmosphere in the presence of base (K_2CO_3). (B) Ullmann homo-coupling of methyl 4-iodobenzoate ($Ar'-I$) proceeds under UV-vis light irradiation in the presence of catalyst ($Pd@TiO_2$) and base (Cs_2CO_3) utilizing tetrahydrofuran (THF) as solvent and Ar atmosphere. (C) Alkene isomerization⁸ of estragole can be carried out upon blue light irradiation of a methanolic suspension of $Pd@TiO_2$ under argon atmosphere. (D) Alkene hydrogenation of estragole can be performed under the isomerization conditions by switching the light to UV light.

reaction shows great catalyst recyclability and is a plausible recovery reaction; as illustrated in Fig. 1. Note that we use the word 'deterioration' rather than the more conventional 'poisoning'; the latter suggests contamination by some unwanted material, while deterioration seems a broader description, perhaps more suitable in this case where the results suggest that changes in the oxidation state of palladium (*vide infra*) may be behind the reduced catalyst performance.

Inspired by the crop rotation process utilized in agriculture, we realized the importance of understanding the reaction mechanism as well as the properties of the catalytic material used. Mechanistically the reactions of Scheme 1 involve electron-hole charge separation when irradiated in the UVA region and direct excitation of the Pd nanoparticles when visible light is used (Scheme 2). Further details appear in earlier publications.⁶⁻⁸ It is important to highlight that the solvents used for



Scheme 2 Suggested mechanisms under UVA (A) or visible (B) irradiation. (A) Upon UVA excitation an electron is pumped from the valence band (VB) into the conduction band (CB) of the semiconductor (TiO_2). The electron can be trapped by the Pd nanoparticle attached to the surface slowing down the electron-hole recombination kinetics. Therefore, electron acceptor reagents (EA) can react more easily on the catalyst surface whereas a sacrificial electron donor (SED), frequently the solvent, quenches the hole. (B) Under visible light excitation, the generation of hot electrons on the Pd surface can photocatalyze reactions through (1) local heat generation or (2) hot electron transfer (eT),¹² the latter being the accepted mechanism for this type of non-plasmonic nanoparticles.

each reaction play an important role on the activity and reusability of this catalyst, actively participating in the reaction mechanism.

A closer look to Sonogashira reaction has shown⁷ that the decreased catalytic performance indicated in reaction A (Scheme 1) is not due to the leaching of Pd species from $Pd@TiO_2$; in fact, ICP measurements revealed that >97% of the Pd is retained by the catalyst after three reaction cycles. Further, the reaction supernatant shows no catalytic activity after separation from the solid catalyst, reinforcing the heterogeneous nature of the reaction.⁷ Material characterization showed that particle size is not altered during the catalytic processes.

With all this in mind, we decided to perform XPS analyses of the materials. One can observe that the HR-XPS spectrum of Pd changes after the first cycle of Sonogashira reaction. These changes, illustrated in Fig. 2A and B are consistent with changes in the oxidation state of Pd on the catalyst surface. For instance, XPS analysis of the fresh catalyst suggests the presence of PdO ,⁸ with a small contribution of more reduced palladium species. In contrast, more reduced Pd species are found after the first use of the catalyst for the Sonogashira reaction. This change accompanies the loss of activity after the first catalytic cycle. Interestingly, after performing the Ullmann reaction there is less contribution of the reduced Pd species, with less dramatic changes comparing to the fresh material (Fig. 2C), consistent with the great reusability for this reaction. To our surprise, photochemical treatment with THF – the solvent used during Ullmann coupling – restores the oxidation state of Pd to almost the same as in the fresh material, Fig. 2D. This is in agreement with our previous studies over thermal alkene isomerizations⁸ utilizing the same catalyst, where we reported the oxidation of Pd species during the catalytic reaction. We then described photocatalytic treatments performed over used $Pd@TiO_2$ catalyst with complete recovery of the catalyst efficiency.^{7,8} Thus, oxidation changes of the Pd surface provide a plausible rationalization for catalyst deterioration, reductive treatments –

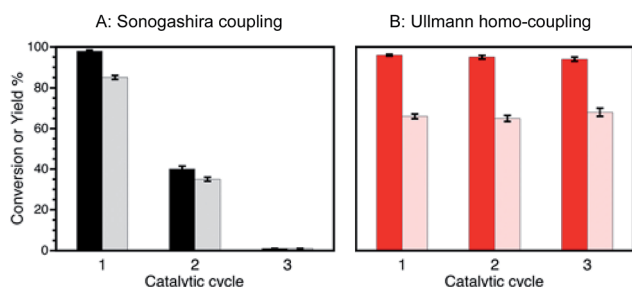


Fig. 1 Conversions (dark bars) and yields (light bars) obtained after several catalytic cycles of reactions (A) and (B) in Scheme 1. While reaction (A) experiences a dramatic efficiency drop, reaction (B) can be catalyzed with excellent conversions and yields for several catalytic cycles. Reaction conditions: (A) Sonogashira coupling upon 450 nm irradiation at 2.7 W cm^{-2} , (B) Ullmann homo-coupling upon 368 nm and 465 nm irradiation at 0.3 and 1.6 W cm^{-2} , respectively.



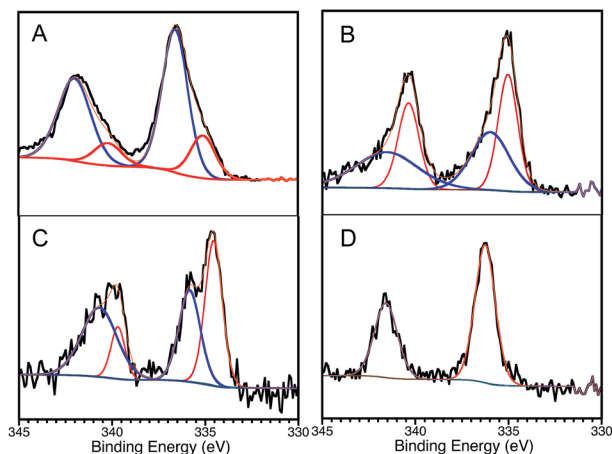


Fig. 2 Pd 3d HR-XPS spectra for Pd@TiO₂ catalyst. (A) Fresh catalyst: Pd 3d core-level spectrum deconvoluted by using two spin-orbit split Pd 3d_{5/2} and Pd 3d_{3/2} components centered at 336.6 eV and 342.0 eV and separated by ~5.4 eV; attributed to PdO.⁸ Small contribution of more reduced palladium species are also found on the material (components at 335.1 eV and 340.2 eV). (B) Catalyst after Sonogashira reaction: high contribution of more reduced species (spin-orbit components at 335.0 (336.0) eV and 340.4 (341.5) eV). (C) Catalyst after Ullmann reaction: similar contribution of both oxidized and less oxidized species. (D) Catalyst after Sonogashira reaction and post-treatment with THF: oxidation state of Pd restored to almost the same as in the fresh material (336.1 and 341.5 eV).

such as irradiation in the presence of a reductive benzoin photoinitiator (I-2959) – completely recovered the catalytic activity.⁸

Considering these observations, we designed a series of different reaction rotations where one would expect the most efficient reactions (Ullmann C–C coupling) would help to improve the efficiencies of the poor ones (Sonogashira C–C coupling). After screening the reaction-rotation conditions – similar to what happens in agriculture – we found the right combination of reactions. Accordingly, rotation with Ullmann reaction remarkably improves the efficiency of the catalyst towards Sonogashira coupling (Fig. 3), with up to 80% yield (1 h) after 6 catalytic cycles, ESI Table S1.† Clearly the Ullmann reaction assists in maintaining the catalyst performance in the Sonogashira reaction. In the same series of experiments (see ESI Table S2†) we show that it is not essential to always alternate the reactions, and that two of the same kind can be performed in sequence.

We were also able to establish that the catalytic farming strategy can be further expanded to additional reactions. Thus, reactions, such as alkene isomerization or hydrogenation, Scheme 1,⁸ can contribute to the catalytic farming strategy while retaining catalyst performance. Accordingly, reaction (C) (or (D)) when run independently, can be catalyzed with excellent conversions and yields for several catalytic cycles (Fig. 4).

The addition of the isomerization reaction serves to illustrate the robustness of the reaction rotation strategy. While alkene isomerization does not restore the catalytic activity toward Sonogashira reaction, its inclusion in the catalytic farming process does not alter the performance of Sonogashira C–C

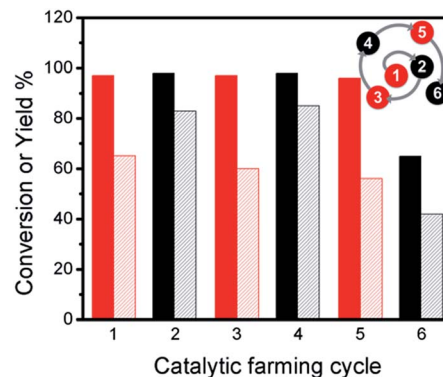


Fig. 3 Conversions (dark bars) and yields (light bars) for catalytic farming of Pd@TiO₂ by rotation between Sonogashira coupling (black) upon 450 nm irradiation at 2.7 W cm⁻² for 30 min and Ullmann homo-coupling (red) upon 368 nm and 465 nm irradiation at 0.3 and 1.6 W cm⁻² for 1 h. Compare to Fig. 1A and B. The spiral at the top-right corner helps us visualize the sequence of reactions with the number representing the reaction sequence, and the color the type of reaction. Similar spirals are included in other figures.

coupling (Fig. 5). In the cases of Fig. 5 it is clear that the Ullmann reaction plays an important role in extending the catalyst lifetime. As already noted, alkene isomerization deactivates the catalyst towards Sonogashira coupling, Fig. 5A, whereas Sonogashira coupling partially retains the catalyst activity towards alkene isomerization. Hence, in the crop rotation analogy, Sonogashira coupling cannot follow isomerization. Likewise, the alkene isomerization is drastically decreased if used as an in-between reaction (Fig. 5 B), however this reaction does not affect the performance of Ullmann as a subsequent reaction (Fig. 5C). Further, Sonogashira coupling shows excellent reactivity in catalytic cycles 4th and 5th with excellent TON numbers (2037 and 2011 TON per Pd NP, respectively – see ESI Table S3†). Notice that the rotation outcome also depends on the irradiation conditions; hence, when using lower irradiation intensities, Sonogashira coupling is only partially deactivated by the alkene isomerization reaction (see ESI Table S4†). Similar results are found when using alkene hydrogenation reaction (see ESI Table S5†). Notice that under these conditions after 6 catalytic cycles, the Ullmann reaction no longer serves as

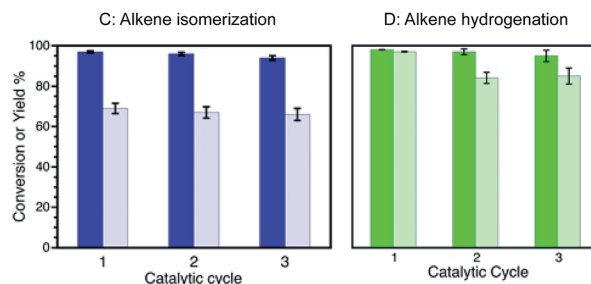


Fig. 4 Conversions (dark bars) and yields (light bars) obtained after several catalytic cycles of (C) alkene isomerization upon 450 nm irradiation at 2.7 W cm⁻² and (D) alkene hydrogenation upon 368 nm irradiation at 0.3 W cm⁻². Notice that each catalytic cycle implies catalyst separation – cleaning cycles – before reusability test.



a fixed set of reactants. It helps in reducing catalyst deterioration and increases longevity and product yield.

The set of reactions, catalyst, and rotation sequence will depend on the synthetic goals of a given laboratory or organization. Once again, the analogy with agriculture is very enlightening. When 16 farmers in one region were asked to provide their favorite crop rotation strategy, they provided 16 different answers, where some crop rotations make frequent appearances (rye, alfalfa, garlic).¹⁴ Just as in chemistry, there is no perfect rotation sequence, as external parameters must be considered, including the usefulness of the crop or target product, and in our case, consideration that one reaction may play a key role in maintaining catalyst (“soil”) performance. Therefore, different laboratories may create rotation sequences that meet their needs, involving some reactions included mainly for catalyst reactivation, such as the catalyst irradiation in THF in the case above.

Experimental section

Materials

Unless otherwise specified, all chemicals were purchased from Sigma-Aldrich or Fisher Scientific and used without further purification. Titanium dioxide (TiO₂-P25) was purchased from Univar Canada. All solvents were of HPLC grade.

Instrumentation

Transmission electron microscopy (TEM) images were collected on a JEM-2100F FETEM (JEOL) operating at 200 kV. The Pd content of the catalysts was determined by Inductively Coupled Plasma Optical Emission Spectrometry (ICP-OES), using Agilent 5110 ICP-OES instrument. Approximately 10 mg portions were accurately weighed in triplicate and digested with aqua regia. Solutions were further diluted and measured by ICP-OES. The Pd 340.458 nm emission line was used for quantification. The XPS spectra were measured on a Kratos Nova AXIS spectrometer equipped with an Al X-ray source. The XPS data were collected using AlK α radiation at 1486.69 eV (150 W, 15 kV), charge neutralizer and a delay-line detector (DLD) consisting of three multi-channel plates. Binding energies are referred to the C 1s peak at 284.8 eV. XPS data was analyzed using CasaXPS software, Version 2.3.15 and all fittings obtained using a Gaussian 30% Laurentian and a Shirley baseline. UV irradiation used for catalyst synthesis was performed in a Luzchem photoreactor equipped with UVA lamps (typically operated with 14 lamps, corresponding to ~ 0.029 W cm⁻² with $\sim 4\%$ spectral contamination. Light-emitting diodes (centered at 368 and 465 nm, respectively) of 10 W from LedEngin and Luzchem LED illuminator (LEDi) equipped with a head of seven powerful blue LEDs (centered at 450 nm) with adjustable intensity at focal point were used as described for the photocatalytic reactions studied. Quantification was carried out in a Perkin Elmer, Claurus Gas Chromatograph coupled to a Flame Ionization Detector (FID) and a DB-5 column (30 m length, 0.320 mm diameter, 0.25 μ m film) using Ar as a carrier gas and *t*-Butyl benzene as external standard. GC-MS analyses were performed

on an Agilent 6890-N Gas Chromatograph with an Agilent 5973 mass selective detector calibrated with acetophenone.

Catalyst synthesis

Palladium nanoparticles (~ 2 wt%) supported on TiO₂ (Pd@TiO₂), were prepared by photodeposition of PdNP onto TiO₂ (P25) and fully characterized as described in our previous report.⁸

Sonogashira C–C coupling

Visible light-induced Sonogashira C–C coupling was performed as described in our previous report.⁷ In brief, 15 mg of Pd@TiO₂ were dispersed in 4 mL of HPLC grade methanol (MeOH) in a 10 mL clean tube, then 15 μ L of iodobenzene (1 eq., 0.13 mmol), 18 μ L of phenylacetylene (1.3 eq., 0.16 mmol) and 35 mg of K₂CO₃ (2 eq., 0.26 mmol), were added. The reaction mixture was purged with Ar for 15 min then irradiated with 1×465 nm LED set up at 1.6 W cm⁻² for 5 h (or 7×450 nm LEDs set up at 2.7 W cm⁻² for 30 min) under continuous stirring. The solid catalyst was separated by centrifugation. Quantification was done by GC-FID using *t*-butyl benzene as an external standard (see ESI Table S7[†]).

Alkene isomerization/hydrogenation

Visible light-induced isomerization (or hydrogenation) of estragole was performed with slight modifications to our previous report.⁷ In brief, 15 mg of Pd@TiO₂ were dispersed in 4 mL of HPLC grade MeOH in a clean quartz cuvette, then 25 μ L (0.16 mmol) of estragole were added. The reaction mixture was purged with Ar for 15 min and then irradiated with 7×450 nm LEDs set up at 2.7 W cm⁻² for 5 h under continuous stirring (or with 1×368 nm LED set up at 0.3 W cm⁻² for hydrogenation). The progress of the reaction was monitored by GC-MS. The quantification was done by GC-FID using *t*-butyl benzene as an external standard (see ESI Table S8[†]).

Ullmann homo-coupling

Light-induced Ullmann homo-coupling of methyl 4-iodobenzoate was carried out based on our recent publication.⁶ 20 mg Pd@TiO₂ were dispersed in 4 mL of tetrahydrofuran (THF) in a clean quartz tube, then 26 mg (0.1 mmol, 1 eq.) of methyl-4 iodobenzoate and 65 mg (0.2 mmol, 2 eq.) of Cs₂CO₃ were added. The reaction mixture was purged with Ar for 10 min prior to irradiation. Irradiation sources used: 1×465 nm LED plus 1×368 nm LED set up at 1.6 and 0.3 W cm⁻², respectively; or 1×368 nm LED set up at 0.3 W cm⁻². The progress of the reaction and the quantification were done by GC-FID using *t*-butyl benzene as an external standard (see ESI Table S9[†]).

Catalyst recyclability

The catalyst was recovered after each cycle by centrifugation (3500 rpm for 15 min). Once the supernatant was decanted, the catalyst was washed three times with ~ 6 mL fresh methanol. Each time the catalyst was dispersed *via* sonication and isolated through centrifugation. The recovered clean catalyst was



suspended in 4 mL HPLC grade MeOH in a clean tube prior to reuse. Reactant concentrations and irradiation time were kept constant for all the cycles and catalyst losses during the recovery process were considered negligible.

Catalyst recovery treatment

The recovered catalyst from two subsequent cycles of light-induced Sonogashira reaction was separated from the reaction mixture by centrifugation (3500 rpm for 15 min). In the recovery process the catalyst was washed 2 times with ~5 mL fresh MeOH then 2 more times with ~5 mL fresh THF prior to activation. In brief, the recovered Pd@TiO₂ was added to 4 mL THF and 60 mg Cs₂CO₃ into a clean quartz tube, suspended by sonication for 10 min then purged with Ar for 15 min prior to 368/465 nm irradiation for ~1 h. The activated solid catalyst was separated by centrifugation, washed with MeOH three times prior to use for a new cycle for light-induced Sonogashira coupling reaction. Catalyst reactivation using the benzoin photoinitiator (I-2959) was performed as previously reported.⁸

Catalytic farming

The reaction was scaled up twice to facilitate catalyst recovery and reuse. The catalyst was recovered after each cycle by centrifugation (3500 rpm for 15 min). After each cycle the catalyst was dispersed in fresh clean solvent *via* sonication and isolated through centrifugation for at least 3 times, and finally dried. Reactions were carried out at given conditions (see figure captions).

Turnover number (TON) and turnover frequency (TOF) calculations¹⁵

Considering that each PdNP has at least one catalytic active site, the TON and TOF are calculated related to the moles of PdNPs as follows:

$$\text{TON} = \frac{\text{moles of reagent} \times \text{yield}}{\text{moles of Pd NP}(n)}$$

where the moles of PdNPs (n) are calculated as follows:

$$n = \frac{\text{mass of catalyst} \times \text{wt}\% \text{ Pd}}{\text{AW} \times \text{number of Pd atoms per NP}(N)}$$

and N is the number of Pd atoms per nanoparticle and AW the atomic weight:

$$N = \frac{\text{Pd NP volume}}{\text{Pd atomic volume}}$$

TOF in h⁻¹

$$\text{TOF} = \frac{\text{TON}}{\text{Time of reaction}(h)}$$

Conclusions

In this contribution we propose a new approach to extend catalyst lifetimes based on the crop rotation system used in agriculture rotation practices may become a standard strategy in heterogeneous catalysis, just as they do in organic farming. While this contribution demonstrates the benefits of rotation in catalysis, we also recognize that practical applications in industry will have to meet market demands as a consideration in reaction rotation. Both represent changes in societal attitudes that recognize and celebrate the use of sustainable practices.

Conflicts of interest

There are no conflicts to declare.

Acknowledgements

This work was supported by the Natural Sciences and Engineering Research Council of Canada, the Canada Foundation for Innovation, and the Canada Research Chairs Program.

References

- 1 A. Biffis, P. Centomo, A. Del Zotto and M. Zeccal, *Chem. Rev.*, 2018, **118**, 2249.
- 2 (a) Q. Liu, M. D. Xu, J. Zhao, Z. Yang, C. Z. Qi, M. F. Zeng, R. Xia, X. Z. Cao and B. Y. Wang, *Int. J. Biol. Macromol.*, 2018, **113**, 1308; (b) M. F. Zeng, X. Zhang, L. J. Shao, C. Z. Qi and X. M. Zhang, *J. Organomet. Chem.*, 2012, **704**, 29; (c) Z. P. Chen, E. Vorobyeva, S. Mitchell, E. Fako, M. A. Ortuno, N. Lopez, S. M. Collins, P. A. Midgley, S. Richard, G. Vile and J. Perez-Ramirez, *Nat. Nanotechnol.*, 2018, **13**, 702.
- 3 (a) C. M. Friend and B. Xu, *Acc. Chem. Res.*, 2017, **50**, 517; (b) W. P. Gao, Z. D. Hood and M. F. Chi, *Acc. Chem. Res.*, 2017, **50**, 787; (c) A. Corma and H. Garcia, *Chem. Soc. Rev.*, 2008, **37**, 2096; (d) A. Corma, R. Juarez, M. Boronat, F. Sanchez, M. Iglesias and H. Garcia, *Chem. Commun.*, 2011, **47**, 1446.
- 4 M. Argyle and C. Bartholomew, *Catalysts*, 2015, **5**, 145.
- 5 A. Akcil, F. Veglio, F. Ferella, M. D. Okudan and A. Tuncuk, *J. Waste Manage.*, 2015, **45**, 420.
- 6 N. Marina, A. E. Lanterna and J. C. Scaiano, *ACS Catal.*, 2018, 7593.
- 7 A. Elhage, A. E. Lanterna and J. C. Scaiano, *ACS Sustainable Chem. Eng.*, 2018, **6**, 1717.
- 8 A. Elhage, A. E. Lanterna and J. C. Scaiano, *ACS Catal.*, 2017, **7**, 250.
- 9 The electronic Rothamsted Documents Archive, <http://www.era.rothamsted.ac.uk>, Accessed April, 2018.
- 10 *Crop Rotation on Organic Farms: A Planning Manual ed.*, ed. C. I. Mohler and S. E. Johnson, Natural Resource, Agriculture, and Engineering Service, Ithaca, NY, USA, 2009.



- 11 P. Anastas and N. Eghbali, *Chem. Soc. Rev.*, 2010, **39**, 301.
- 12 (a) S. Sarina, E. Jaatinen, Q. Xiao, Y. M. Huang, P. Christopher, J. C. Zhao and H. Y. Zhu, *Chem. Phys. Lett.*, 2017, **8**, 2526; (b) T. Tana, X. W. Guo, Q. Xiao, Y. M. Huang, S. Sarina, P. Christopher, J. F. Jia, H. S. Wu and H. Y. Zhu, *Chem. Commun.*, 2016, **52**, 11567.
- 13 K. Koehler-Cole, J. R. Brandle, C. A. Francis, C. A. Shapiro, E. E. Blankenship and P. S. Baenziger, *Renew. Agr. Food Syst.*, 2017, **32**, 474.
- 14 I. R. Chongtham, G. Bergkvist, C. A. Watson, E. Sandstrom, J. Bengtsson and I. Oborn, *Biol. Agric. Hortic.*, 2017, **33**, 14.
- 15 G. K. Hodgson and J. C. Scaiano, *ACS Catal.*, 2018, **8**, 2914.

